

Low-lying energy levels of $^{229}\text{Th}^{35+}$ and the electronic bridge process

S. G. Porsev^{1,2}, C. Cheung¹, and M. S. Safronova¹

¹*Department of Physics and Astronomy, University of Delaware, Newark, Delaware 19716, USA*

²*Petersburg Nuclear Physics Institute of NRC “Kurchatov Institute”, Gatchina, Leningrad district 188300, Russia*

The nuclear transition between the ground and the low-energy isomeric state in the ^{229}Th nucleus is of interest due to its high sensitivity to a hypothetical temporal variation of the fundamental constants and a possibility to build a very precise nuclear clock, but precise knowledge of the nuclear clock transition frequency is required. In this work we estimate the probability of an electronic bridge process in $^{229}\text{Th}^{35+}$, allowing to determine the nuclear transition frequency and reduce its uncertainty. Using configuration interaction methods we calculated energies of the low-lying states of Th^{35+} and determined their uncertainties.

I. INTRODUCTION

A specific feature of the ^{229}Th nucleus is that the energy difference between the ground state and the first excited state is only several eV. An existence of such a low-lying level was established more than forty years ago [1], but a precise measurement of the isomeric state energy turned out to be very difficult. In 1994 Helmer and Reich [2] measured this excitation energy (ω_N) to be 3.5 ± 1 eV. In Ref. [3] it was obtained as 5.5 ± 1.0 eV. The experiments of Beck *et al.* [4, 5] gave an even larger value with less error, $\omega_N = 7.8 \pm 0.5$ eV. Finally, in recent experiments of Seiferle *et al.* [6] and Sikorsky *et al.* [7] the values $\omega_N = 8.28 \pm 0.17$ and $\omega_N = 8.10 \pm 0.17$ eV were obtained. Both these results were used in an analysis carried out in Ref. [8] yielding the value $\omega_N = 8.19 \pm 0.12$ eV. Thus, the current most precise value differs from the result of 1994 by more than two times, but is in a good agreement with the result obtained in Ref. [5].

The nuclear transition between the ground and the low-energy isomeric state in the ^{229}Th nucleus is of interest due to its high sensitivity to a hypothetical temporal variation of the fundamental constants [9]. Another unique feature of this transition is a possibility to build a very precise nuclear clock [10]. It requires the precise knowledge of the nuclear clock transition frequency and, consequently, further investigations aiming to refine the value of ω_N are needed.

An experimental progress in trapping and sympathetic cooling of highly charged ions (HCIs) (see review in Ref. [11] for details) using electron-beam ion traps (EBITs) opened new possibilities to use optical transitions of such ions for different applications. As it was discussed in Ref. [11], an interaction region of an electron beam with maximum magnetic field in EBITs is short enough that reduces possible electron-beam instabilities and also allows for a high charge density. Both of these effects speed up the ionization process. If a highly charged ion, considered as a clock candidate, does not have a transition suitable for laser cooling, sympathetic cooling can be done by trapping the HCI together with the cooling ion in the same trapping potential and using their mutual Coulomb interaction. In the recent paper [12] it was suggested to use the electronic bridge (EB) process

in Th^{35+} for an accurate determination of the nuclear isomeric energy and the energies of the low-lying states, needed to estimate the EB process rate, were calculated.

Since the EB process rate depends drastically on the energies of the states involved in this process, we calculated the energies of the low-lying states of Th^{35+} in different approximations of increasing complexity. The main configuration of the ground state of the ion is $(1s^2 \dots 4d^{10} 4f^9)$ and we used configuration interaction (CI) method for calculations. First, we performed a 9-electron CI calculation, including nine $4f$ electrons in the valence field while treating all other electrons as the core electrons. Then, we carried out 19- and 25-electron CI calculations, including the $4f, 4d$ and $4f, 4d, 4p$ electrons into the valence field, respectively. In such a way we were able to estimate the role of core-valence correlations, what allowed us to determine the uncertainties of the energies.

To carry out these calculations for such a complicated open-shell system as Th^{35+} we used a new parallel atomic structure code package developed and described in Ref. [13]. This package (i) allows us much quicker computations and (ii) enables to work with a CI space of a much larger size than was possible previously when we used serial versions of the programs. Using a parallel version of the program for the CI calculation, we were able to use several hundreds of processors simultaneously and, consequently, to work with a large CI space, involving up to 120 millions of determinants.

Using the energies obtained and assuming a resonant character of the induced EB process, we estimated its rate for several possible values of the nuclear isomeric energy. Based on these calculations we conclude that modern facilities of EBITs and available ultra-violet lasers allow us to determine more precisely the nuclear isomeric energy and reduce its uncertainty.

II. ELECTRONIC BRIDGE EXCITATION

Here we consider the process of the excitation of the nucleus from the ground (g) to the isomeric state (m) by an electronic bridge process driven by a one-photon excitation of the electron shell. Such a process, relying on

the absorption of an incident photon, can be represented by the Feynman diagram in Fig. 1. In this process the electronic shell is promoted by a laser photon from its initial state t to an excited state k and then decays to a lower-lying state i . The energy transferred to the nucleus is used to excite it from the ground to isomeric state. Assuming a resonant character of the process, we take into account only one Feynman diagram that gives the main contribution to the probability of the process.

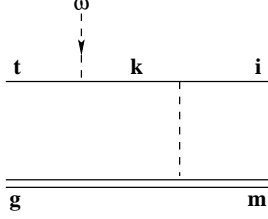


FIG. 1. The Feynman diagram of the considered electronic bridge process. The single and double solid lines relate to the electronic and the nuclear transitions, correspondingly. The dashed line is the photon line.

In the following we use the formalism developed in Refs. [14–16] with the difference that an $M1$ photon (instead of a $E1$ photon) is absorbed by the electron shell. Such a photon is described by the magnetic moment operator

$$\boldsymbol{\mu} = -\mu_0 (\mathbf{J} + \mathbf{S}). \quad (1)$$

Here \mathbf{J} and \mathbf{S} are the total and spin momentum operators and μ_0 is the Bohr magneton determined as $\mu_0 = |e|\hbar/(2mc)$, where e and m is the electron charge and mass, c is the speed of light, and \hbar is the Plank constant. (If not stated otherwise the atomic units $\hbar = m = |e| = 1$ and $c \approx 137$ are used in the following).

We assume that the incident radiation with spectral intensity I_ω is isotropic and unpolarized. Following Ref. [17] the relation between the EB excitation rate, Γ_{exc} , and the rate of the inverse spontaneous EB process, Γ , that can be formally described by the mirror-image of Fig. 1 with an outgoing photon arrow, can be written as

$$\Gamma_{\text{exc}} = \Gamma \frac{4\pi^3 c^2}{\omega^3} g_r I_\omega, \quad (2)$$

where ω is the frequency of the absorbed photon. The factor $g_r \equiv (2I_m + 1)(2J_i + 1)/[(2I_g + 1)(2J_t + 1)]$ appears because we average over the initial projections and summing over the final projections of the electronic and nuclear total angular momenta. Here I_m (I_g) is the nuclear spin of the isomeric (ground) state and J_i (J_t) is the total angular momentum of the initial (final) electronic state in the spontaneous EB process.

The general expression for the probability of the EB process was derived in Ref. [15]. Assuming a resonance character of the spontaneous EB process, its transition

rate can be written as,

$$\Gamma \approx \frac{16\pi}{3(2J_i + 1)} \left(\frac{\omega}{c}\right)^3 \sum_{K=1}^2 \frac{B(\tau K) G_K}{(2K + 1)^2}. \quad (3)$$

The reduced probabilities, $B(M1)$ and $B(E2)$, of the nuclear magnetic-dipole and electric-quadrupole $m \rightarrow g$ transition are determined as

$$B(\tau K) = \frac{1}{2I_m + 1} \frac{2K + 1}{4\pi} |\langle I_g || \mathcal{M}_K || I_m \rangle|^2, \quad (4)$$

where $\tau \equiv M$ for $K = 1$ and $\tau \equiv E$ for $K = 2$; \mathcal{M}_1 and \mathcal{M}_2 are the magnetic-dipole and electric-quadrupole nuclear moment operators, and $|I_g\rangle = 5/2^+$ [633] and $|I_m\rangle = 3/2^+$ [631] are the ground and isomeric nuclear states, respectively, given in their Nilsson classification.

The explicit expression for the quantity G_K was derived in Ref. [15] and in our case is reduced to

$$G_K \approx \frac{1}{2J_k + 1} \left| \frac{\langle i || T_K || k \rangle \langle k || \boldsymbol{\mu} || t \rangle}{E_k - E_i - \omega_N} \right|^2, \quad (5)$$

where $|i\rangle$, $|k\rangle$, and $|t\rangle$ are the electronic states, E_k and E_i are the energies of the respective states, J_k is the electron total angular momentum of the state $|k\rangle$, and ω_N is the nuclear transition frequency. We assume that there is only one state giving the dominant contribution to G_K , while the contribution of all other intermediate states is negligible, i.e., the state $|k\rangle$ is chosen so that $E_k - E_i \approx \omega_N$.

The expressions for the single-electron operators T_1 and T_2 can be written as

$$\begin{aligned} T_{1\lambda}(\mathbf{r}) &= -\frac{i\sqrt{2}\boldsymbol{\alpha} \cdot \mathbf{C}_{1\lambda}^{(0)}(\mathbf{n})}{c r^2}, \\ T_{2\lambda}(\mathbf{r}) &= -\frac{C_{2\lambda}(\mathbf{n})}{r^3}, \end{aligned} \quad (6)$$

where $\boldsymbol{\alpha}$ is the Dirac matrix, $\mathbf{n} \equiv \mathbf{r}/r$, and $\mathbf{C}_{K\lambda}^{(0)}$ is a normalized vector spherical harmonic defined by (see, e.g., Ref. [18])

$$\mathbf{C}_{K\lambda}^{(0)}(\mathbf{n}) = \frac{\mathbf{L}}{\sqrt{K(K+1)}} C_{K\lambda}(\mathbf{n}). \quad (7)$$

Here \mathbf{L} is the orbital angular-momentum operator and $C_{K\lambda}$ is a spherical harmonic given by

$$C_{K\lambda}(\mathbf{n}) = \sqrt{\frac{4\pi}{2K+1}} Y_{K\lambda}(\mathbf{n}). \quad (8)$$

A most accurate determination of the nuclear transition frequency ω_N was recently done in Ref. [8] to be $\omega_N = 8.19(12)$ eV. The authors of Ref. [12] calculated the low-lying energy levels of Th^{35+} and found the transition frequency from the low-lying excited state with $J = 13/2$ to the ground state ($J = 15/2$) to be 8.40 eV which is close to ω_N . The state with $J = 11/2$ and $E \approx 4.2$ eV can be used as the initial state in the induced

EB process. Applying the designations in Fig. 1 we have $|t\rangle \equiv |J = 11/2\rangle$, $|k\rangle \equiv |J = 13/2\rangle$, and $|i\rangle \equiv |J = 15/2\rangle$.

We carried out the calculation of the low-lying states in the framework of the CI method using the program package described in Ref. [19] and further developed in Ref. [13]. We included the Breit interaction correction and estimated the core-valence correlations. Our results, discussed more detailed in the following sections, confirmed the main conclusion of Ref. [12] about a possibility to determine accurately the nuclear isomer energy using the EB process with realistic laser parameters.

III. METHOD OF CALCULATION AND RESULTS.

We start calculations of energy levels of Th^{35+} belonging to the $(1s^2, \dots, 4f^9)$ configuration from solution of the Dirac-Hartree-Fock (DHF) equations, carrying out a self-consistency procedure for the $[1s^2, \dots, 4f^9]$ electrons. The Breit interaction was included in this procedure. The remaining virtual orbitals were formed using a recurrent procedure described in [19, 20], when the large component of the radial Dirac bispinor, $f_{n'l'j'}$, was obtained from a previously constructed function f_{nlj} by multiplying it to $r^{l'-l} \sin(kr)$, where l' and l are the orbital quantum numbers of the new and old orbitals ($l' \geq l$) and the coefficient k is determined by the properties of the radial grid. The small component $g_{n'l'j'}$ was found from the kinetic balance condition:

$$g_{n'l'j'} = \frac{\sigma \mathbf{p}}{2mc} f_{n'l'j'}, \quad (9)$$

where σ are the Pauli matrices, \mathbf{p} and m are the electron momentum and mass, and c is the speed of light. The newly constructed functions were then orthonormalized with respect to the functions of the same symmetry. In constructing the virtual orbitals we did not diagonalize the basis set.

In total the basis set consisted of six partial waves ($l \leq 5$) including the orbitals up to $10s$, $10p$, $10d$, $10f$, $10g$, and $10h$. The configuration space grows very rapidly with an increase of the basis set; for this reason the basis set is rather short.

For an accurate calculation of energies we need to take into account valence-valence and core-valence correlations. The former can be treated explicitly in the framework of the CI method. A CI many-electron wave function of a given angular momentum J and parity can be represented by a linear combination of Slater determinants [21]:

$$\Psi_J = \sum_k a_k \Phi_k. \quad (10)$$

A way to account for core-valence correlations was suggested in Ref. [21], but in practice it is applicable when the number of valence electrons does not exceed 4-5. In our consideration we include nine $4f$ electrons into the

valence field and such a method is impractical. To estimate the role of different core shells, we carried out several calculations of increasing complexity in the framework of the CI method sequentially adding the core shells into the valence field. In this way we carried out the 9-, 19- and 25-electron CI calculations when the $4f$, $(4f, 4d)$, and $(4f, 4d, 4p)$, electrons, respectively, were included in the CI space. Below we discuss these calculations more detailed.

A. 9-electron CI

We start from the most simple case of the 9-electron CI. To check the convergence of the CI method, we calculated the low-lying energy levels for five cases. In the first case we included the single and double excitations of the electrons from the main configuration $4f^9$ to the $6s$, $6p$, $6d$, $6f$, $6g$ and $6h$ orbitals (we designate it as $[6spdfgh]$). In other four calculations, we included the single and double excitations to $[nspdfgh]$, where $n = 7 - 10$. We checked that an inclusion of the triple excitations change the energies only by few cm^{-1} . Thus, this contribution can be neglected.

The results are presented in Table I. The terms are determined by their total angular momentum J . The energies of four lowest-lying excited states counted from the ground state and found for different n (when the single and double excitations were allowed to $[nspdfgh]$) are presented in the columns labeled “ E ” in cm^{-1} . The energy differences $\Delta(n) \equiv E(nspdfgh) - E(n-1spdfgh)$ and the ratios $\delta_n \equiv \Delta(n)/\Delta(n-1)$ are given in the columns labeled “ $\Delta(n)$ ” (in cm^{-1}) and “ δ_n ”. The total values are given in the last row.

To estimate the contribution to the energies from the configurations containing shells with $n > 10$, we note that δ_n for $n = 8, 9, 10$ are numerically close to each other for all terms. Assuming that the same is true and for $n > 10$ we are able to use the formula for a geometric progression to estimate the respective contribution.

Putting the first term of the geometric progression to be $b_1 \equiv \Delta(7)$, determining q as an average over δ_n for $n = 8, 9, 10$, i.e., $q \equiv (\delta_8 + \delta_9 + \delta_{10})/3$, and using the equation for the sum of k terms in the geometric progression,

$$S_k = \frac{b_1 (1 - q^k)}{1 - q}, \quad (11)$$

we are able to calculate S_k for any k . Then we can estimate $\Delta(n > 10)$, as

$$\Delta(n > 10) \approx S_k - (\Delta_8 + \Delta_9 + \Delta_{10}). \quad (12)$$

For instance, for the $J = 9/2$ term we have $b_1 = -224 \text{ cm}^{-1}$, $q = 0.50$, and putting k to be equal to 100, we find $S_{100} \approx -448 \text{ cm}^{-1}$ and $\Delta(n > 10) \approx -35 \text{ cm}^{-1}$. Carrying out similar calculations for other term, we find the values listed in the row labeled “ $n > 10$ ” of Table I. The total values, obtained as $E(n = 10) + \Delta(n > 10)$, are given in the last row of the table.

TABLE I. 9-electron CI. The energies of four lowest-lying excited states counted from the ground state and found for different n (when the single and double excitations were allowed to $[n\text{spdfgh}]$) are presented in the columns labeled “ E ” in cm^{-1} . The energy differences $E(n\text{spdfgh}) - E(n-1\text{spdfgh})$ are given in the columns labeled “ $\Delta(n)$ ” (in cm^{-1}). The ratios $\Delta(n)/\Delta(n-1)$ are listed in the columns labeled “ δ_n ”. The total values, obtained as $E(n=10) + \Delta(n > 10)$, are given in the last row.

	$J=9/2$			$J=11/2$			$J=3/2$			$J=13/2$		
	E	$\Delta(n)$	δ_n	E	$\Delta(n)$	δ_n	E	$\Delta(n)$	δ_n	E	$\Delta(n)$	δ_n
$n=6$	30503			36728			55006			67200		
$n=7$	30279	-224		36411	-316		54441	-565		67255	54.6	
$n=8$	30171	-108	0.483	36266	-145	0.459	54175	-266	0.471	67290	35.6	0.652
$n=9$	30118	-52.8	0.487	36205	-61.2	0.421	54061	-114	0.430	67313	23.1	0.648
$n=10$	30090	-28.0	0.529	36178	-26.4	0.432	54010	-51.1	0.447	67329	15.9	0.689
q^a			0.500			0.437			0.449			0.663
$n > 10^b$		-35			-13			-29			33	
Total	30055			36165			53980			67362		

^aSee explanation in the text;

^bThe contribution to the energies from the configurations containing shells with $n > 10$.

B. Core-valence correlations

Due to the large number of valence electrons we were unable to apply the method combining the CI with a many-body perturbation theory over residual Coulomb interaction [21] or with linearized coupled-cluster method [22] to find the core-valence correlations. To estimate this contribution to the energies, we additionally performed the 19- and 25-electron CI calculations, including the $4d$ and $4d, 4p$ electrons into the valence field. In both cases we allowed the single and double excitations of the electrons from the all valence shells of the main configuration to $[7\text{spdfgh}]$. For example, for the $4d^{10}4f^9$ main configuration the single and double excitations were allowed from the $4d$ and $4f$ shells. We restricted ourselves by the calculation for $[7\text{spdfgh}]$ because the set of configurations is sufficiently complete in this case and, on the other hand, such a calculation is not extremely demanding to computer resources even for the case of the 25-electron CI.

We focus on computing the energies of the $J = 11/2$ and $J = 13/2$ states that are most important for an accurate calculation of the probability of the EB process, as we discussed in Sec. III. Additionally, if we are interested in only in the states with a large J , it facilitates the CI calculation because it allows us to deal with the CI space of a smaller size. The calculation results of the transition energies obtained for these states in the framework of 9-, 19-, and 25-electron CI calculations with the excitations allowed to $[7\text{spdfg}]$ are presented in Table II. The main configurations of the valence electrons are given in the first column. The energies of the excited states, counted from the ground state energy, are given in the columns labeled “ E ” (in cm^{-1}).

TABLE II. The energies obtained in the framework of 9-, 19-, and 25-electron CI calculations with the excitations allowed to $[7\text{spdfgh}]$, are presented. The main configurations of the valence electrons are given in the first column. The energies of the excited states, counted from the ground state energy, are given in the columns labeled “ E ” (in cm^{-1}). The differences $E(4d^{10}4f^9) - E(4f^9)$ and $E(4p^64d^{10}4f^9) - E(4d^{10}4f^9)$ are given for each state in the column labeled “ Δ ” in cm^{-1} . The sum $\Delta(4d^{10}4f^9) + \Delta(4p^64d^{10}4f^9)$ is presented in the row labeled “Total”.

	$J=11/2$		$J=13/2$	
	E	Δ	E	Δ
$4f^9$	36411		67255	
$4d^{10}4f^9$	37400	989	66948	-307
$4p^64d^{10}4f^9$	37487	87	66899	-49
Total		1076		-356

The differences $\Delta(4d^{10}4f^9) \equiv E(4d^{10}4f^9) - E(4f^9)$ and $\Delta(4p^64d^{10}4f^9) \equiv E(4p^64d^{10}4f^9) - E(4d^{10}4f^9)$ are given for each state in the column labeled “ Δ ” in cm^{-1} . The sum $\Delta(4d^{10}4f^9) + \Delta(4p^64d^{10}4f^9)$ (we designate it as Δ_{Total}) is presented in the row labeled “Total”.

Using the values of the energies from Tables I and II we are able to determine the final value of the energies for the $J = 11/2$ and $J = 13/2$ terms as the sum of the “Total” value given in Table I and Δ_{Total} from Table II. Thus, we finally obtain $E_{J=11/2} \approx 37240(980) \text{ cm}^{-1} \approx 4.62(12) \text{ eV}$ and $E_{J=13/2} \approx 67000(315) \text{ cm}^{-1} \approx 8.307(39) \text{ eV}$.

The uncertainties are mostly determined by the core-valence correlations not taken into account in our consid-

eration. To estimate them we note that $\Delta(4d^{10}4f^9)$ is an order of magnitude smaller than $\Delta(4p^64d^{10}4f^9)$. We assume that a possible contribution from the $[1s-4s]$ core shells to the energies does not exceed $\Delta(4d^{10}4f^9)$ and we estimate the uncertainty of the energy as $|\Delta(4d^{10}4f^9)|$.

Our final values for $E_{J=11/2}$ and $E_{J=13/2}$ can be compared with the results obtained in Ref. [12] to be 4.19 and 8.40 eV, respectively. The difference can be attributed to the Breit correction, omitted in Ref. [12], and a more complete inclusion of the valence-valence and core-valence correlations. In particular, when including the $4d$ shell into the valence field, the authors of Ref. [12] were obliged to reduce the configuration space (due to limitations of the computing facilities) disregarding certain double-electron excitations from the $4d$ shell to the virtual orbitals.

C. EB process excitation rate

Using Eqs. (2-5) we are able to estimate the EB process probability. To find the probability of the spontaneous process given by Eq. (3) we need to calculate the matrix elements (MEs) of the operators T_1 , T_2 , and μ in Eq. (5).

We carried out this calculation for the largest 25-electron CI when single and double excitations were allowed to $[7spdfgh]$ and obtained

$$\begin{aligned} |\langle J = 15/2 || T_1 || J = 13/2 \rangle| &\approx 2.0 \text{ a.u.}, \\ |\langle J = 15/2 || T_2 || J = 13/2 \rangle| &\approx 39 \text{ a.u.}, \\ |\langle J = 13/2 || \mu || J = 11/2 \rangle| &\approx 2.28 \mu_0. \end{aligned} \quad (13)$$

The calculation performed in the framework of the 9-electron CI with allowing single and double excitations to $[10spdfgh]$ led to the values that differ by less than 1% from the results given above.

The values of the reduced probabilities, $B(M1)$ and $B(E2)$, of the nuclear $m \rightarrow g$ transition available in the literature are contradictory. In Ref. [23] the value of $B(M1)$ was found to be 0.048 Weisskopf units (W.u.). The calculation of Ruchowska *et al.* [24] led to the value 0.014 W.u. while the recent model calculation of Minkov and Pálffy [25] predicted the $B(M1)$ value in the limits of 0.005–0.008 W.u., an order of magnitude smaller than the result reported in Ref. [23].

A similar situation arises for $B(E2)$. Strizhov and Tkalya [26], referring to Ref. [27], cited the value of several W.u., while in Ref. [25] it was found an order of magnitude larger value, in the limits 29–43 W.u.. In this work we use for an estimate of the EB transition rate the recent values, $B(M1) = 0.005 \text{ W.u.} \approx 3.5 \times 10^{-14} \text{ a.u.}$ and $B(E2) = 29 \text{ W.u.} \approx 3.1 \times 10^{-16} \text{ a.u.}$, obtained in Ref. [25].

As follows from Eqs. (3-5) the EB transition rate depends substantially from the magnitude of the nuclear transition frequency ω_N determined as 8.19(12) eV in Ref. [8]. To illustrate it we calculated these rates for three values of ω_N : its central value 8.19 eV and two

TABLE III. Possible values of the nuclear transition frequency ω_N are listed in the first column. The quantities G_1 , G_2 , and Γ are given by Eqs. (5) and (3). The values of the EB excitation rate, Γ_{exc} , are presented in the forth column.

ω_N (eV)	G_1 (a.u.)	G_2 (a.u.)	Γ (s ⁻¹)	Γ_{exc} (s ⁻¹)
8.31	1570	5.93×10^5	5.7×10^{-4}	0.3
8.19	1.1	404	3.5×10^{-7}	2.1×10^{-4}
8.07	0.3	99	7.7×10^{-8}	5.0×10^{-5}

edge values of the uncertainty interval 8.31 and 8.07 eV. We note that the frequency of the absorbed photon ω is determined as $\omega = \omega_N - E_{J=11/2}$ and assume that the time-averaged spectral intensity is $I_\omega \simeq 10^{-3} \text{ (W/m}^2\text{) s}$ [12, 14].

The results are presented in Table III. The possible values of the nuclear transition frequency ω_N are listed in the first column. The quantities G_1 , G_2 , and Γ , given by Eqs. (5) and (3), are listed in columns 2-4. We note that for the used values of $B(M1)$ and $B(E2)$, both terms in Eq. (3) give approximately the same contribution. The values of the EB excitation rate per ion, Γ_{exc} , are presented in the fifth column for different ω_N .

As seen from Table III, the largest Γ_{exc} , obtained in the case of $\omega_N = 8.31 \text{ eV}$, reaches 0.3 s^{-1} . This is due to that this value of ω_N is very close to $E_{J=13/2} \approx 8.307 \text{ eV}$ leading to a very small denominator in Eq. (5) and, respectively, very large $G_{1,2}$ and Γ_{exc} . For the other two considered values of the nuclear transition frequency, 8.19 and 8.07 eV, there is no such a resonant enhancement of the effect and the EB excitation rates are several orders of magnitude smaller. Our results are in a reasonable agreement with those obtained in Ref. [12].

IV. CONCLUSION

We carried out the calculation of the low-lying energy levels for such a complicated multivalent ion as Th^{35+} . To determine the contribution of the valence-valence and core-valence correlations, we performed the 9-, 19-, and 25-electron CI calculations, including $4f$, $4f, 4d$, and $4f, 4d, 4p$ shells, respectively, into the valence field. Our calculation showed that the transition energy from the $J = 15/2$ state to the ground state, 8.31 eV, is close to the central value of the experimentally determined nuclear isomer energy, 8.19 eV, and practically coincides with the upper edge value, 8.31 eV. It opens new possibilities for a more precise measurement of the nuclear isomer energy using an electronic bridge process.

We studied a EB process scheme and estimated the excitation rates of the spontaneous and (inverse) induced EB processes for possible values of the $g \rightarrow m$ nuclear transition frequency ω_N . We found the EB excitation rate per ion to be 0.3 s^{-1} in the case of $\omega_N = 8.31 \text{ eV}$.

For other considered values of the nuclear transition frequency, 8.19 and 8.07 eV, this rate is 3-4 orders of magnitude smaller. Based on these results and on the study of Ref. [12] where typical electron beam ion trap conditions were considered, we conclude that an efficient population of the nuclear isomer state and a precise determination of its energy using an EBIT and available ultra-violet lasers is already attainable. The Th^{35+} ion is a very promising candidate for such an experiment.

We are grateful to P. Bilous and A. Pálffy for valuable discussion and useful remarks. This work is a part of the “Thorium Nuclear Clock” project that has received funding from the European Research Council (ERC) under the European Union’s Horizon 2020 research and innovation program (Grant Agreement No. 856415). S.P. acknowledges support by the Russian Science Foundation under Grant No. 19-12-00157. This research was supported in part through the use of the Caviness community cluster at the University of Delaware.

-
- [1] L. A. Kroger and C. W. Reich, Nucl. Phys. A **259**, 29 (1976).
 - [2] R. G. Helmer and C. W. Reich, Phys. Rev. C **49**, 1845 (1994).
 - [3] Z. O. Guimarães-Filho and O. Helene, Phys. Rev. C **71**, 044303 (2005).
 - [4] B. R. Beck, J. A. Becker, P. Beiersdorfer, G. V. Brown, K. J. Moody, J. B. Wilhelmy, F. S. Porter, C. A. Kilbourne, and R. L. Kelley, Phys. Rev. Lett. **98**, 142501 (2007).
 - [5] B. R. Beck, C. Y. Wu, P. Beiersdorfer, G. V. Brown, J. A. Becker, K. J. Moody, J. B. Wilhelmy, F. S. Porter, C. A. Kilbourne, and R. L. Kelley, Improved value for the energy splitting of the ground-state doublet in the nucleus $^{229\text{m}}\text{Th}$, Lawrence Livermore National Laboratory Technical Report No. LLNL-PROC-415170, 2009.
 - [6] B. Seiferle, L. von der Wense, P. V. Bilous, I. Amersdorffer, C. Lemell, F. Libisch, S. Stellmer, T. Schumm, C. E. Düllmann, A. Pálffy, and P. G. Thirolf, Nature (London) **573**, 243 (2019).
 - [7] T. Sikorsky, J. Geist, D. Hengstler, S. Kempf, L. Gastaldo, C. Enss, C. Mokry, J. Runke, C. E. Düllmann, P. Wobrauschek, K. Beeks, V. Rosecker, J. H. Sterba, G. Kazakov, T. Schumm, and A. Fleischmann, Phys. Rev. Lett. **125**, 142503 (2020).
 - [8] E. Peik, T. Schumm, M. Safronova, A. Pálffy, J. Weitenberg, and P. G. Thirolf (accepted to Quantum. Sci. Tech.).
 - [9] E. Peik and C. Tamm, Europhys. Lett. **61**, 181 (2003).
 - [10] V. V. Flambaum, Phys. Rev. Lett. **97**, 092502 (2006).
 - [11] M. G. Kozlov, M. S. Safronova, J. R. Crespo López-Urrutia, and P. O. Schmidt, Rev. Mod. Phys. **90**, 045005 (2018).
 - [12] P. V. Bilous, H. Bekker, J. C. Berengut, B. Seiferle, L. von der Wense, P. G. Thirolf, T. Pfeifer, J. R. C. López-Urrutia, and A. Pálffy, Phys. Rev. Lett. **124**, 192502 (2020).
 - [13] C. Cheung, M. S. Safronova, and S. G. Porsev, Symmetry **13**, 621 (2021).
 - [14] S. G. Porsev, V. V. Flambaum, E. Peik, and C. Tamm, Phys. Rev. Lett. **105**, 182501 (2010).
 - [15] S. G. Porsev and V. V. Flambaum, Phys. Rev. A **81**, 032504 (2010).
 - [16] S. G. Porsev and V. V. Flambaum, Phys. Rev. A **81**, 042516 (2010).
 - [17] I. I. Sobelman, *Atomic Spectra and Radiative Transitions* (Springer-Verlag, Berlin, 1979).
 - [18] D. A. Varshalovich, A. N. Moskalev, and V. K. Khersonskii, *Quantum Theory of Angular Momentum* (World Scientific, Singapore, 1988).
 - [19] M. G. Kozlov, S. G. Porsev, M. S. Safronova, and I. I. Tupitsyn, Comp. Phys. Comm. **195**, 199 (2015).
 - [20] M. G. Kozlov, S. G. Porsev, and V. V. Flambaum, J. Phys. B **29**, 689 (1996).
 - [21] V. A. Dzuba, V. V. Flambaum, and M. G. Kozlov, Phys. Rev. A **54**, 3948 (1996).
 - [22] M. S. Safronova, M. G. Kozlov, W. R. Johnson, and D. Jiang, Phys. Rev. A **80**, 012516 (2009).
 - [23] A. M. Dykhne and E. V. Tkalya, Pis'ma Zh. Eksp. Teor. Fiz. **67**, 233 (1998), [JETP Lett. **67**, 251 (1998)].
 - [24] E. Ruchowska, W. A. Plóciennik, J. Żylicz, H. Mach, J. Kvasil, A. Algora, N. Amzal, T. Bäck, M. G. Borge, R. Boutami, P. A. Butler, J. Cederkäll, B. Cederwall, B. Fogelberg, L. M. Fraile, H. O. U. Fynbo, E. Hagebø, P. Hoff, H. Gausemel, A. Jungclaus, R. Kaczarowski, A. Kerek, W. Kurcewicz, K. Lagergren, E. Nacher, B. Rubio, A. Syntfeld, O. Tengblad, A. A. Wasilewski, and L. Weissman, Phys. Rev. C **73**, 044326 (2006).
 - [25] N. Minkov and A. Pálffy, Phys. Rev. Lett. **122**, 162502 (2019).
 - [26] V. F. Strizhov and E. V. Tkalya, Zh. Eksp. Teor. Fiz. **99**, 697 (1991), [Sov. Phys.-JETP **72**, 387 (1991)].
 - [27] C. E. Bemis, Jr., P. K. McGowan, F. C. Porter *et al.*, Phys. Scr. **38**, 657 (1988).